International Journal of Mechanics and Energy (IJME)
Vol. 7, Issue 1, 2020, ISSN: 2286-5845

Thermo-mechanical behavior analysis of shape memory alloys and estimation of their strain energy absorption, Application to biomechanical technologies

BrahimNecib*, Ali Benhaoua, AbdelazizLebied and Mohamed Sahli
Laboratory of Mechanics (LabMec), Mechanical Engineering Department,
University of FreresMentouri Constantine 1(UFMC1),
Campus ChabErsas, Road of Ain El Bey,25000 Constantine, ALGERIA

Abstract: The shape memory alloys (SMAs) are new materials with remarkable mechanical properties used in many structural technological areas of mechanics, aeronautics or biomechanics. The SMAs are considered to analyze the behavior of cupules of total hip prosthesis reprocessed in a block of polypropylene (PP) extruded in a solid state by using the process of extrusion cranked to equal areas (ECEA). In this work, definitions of SMAs, super elastic effect of shape memory alloys, their construction model and their applications in new technologies will be considered. A thermo mechanical analysis estimation of their strain energy deformation absorption due to external loads has been studded. A predictive model of the behavior induced by simple mechanical stresses is then proposed. This behavior is broken down into two linear parts with two different elastic modules. This analytical modeling is built to be able to estimate the capacity of these alloys to absorb energy of deformation induced by a simple external loading. The Thermo-mechanical parameters of the SMA are determined experimentally. The results reveal differences in absorption of this energy level depending on the State in la when the alloy is located, i.e. martensitic or austenitic phase. The obtained results allowed us to determine the transformation temperatures of different of shape memory alloys materials in one hand, then their Young modules on the other, in order to validate the model of the constitutive behavior of stress deformation. The quantification of the capacity assessment of the SMA to absorb the energy of deformation is therefore essential in order to improve the performance of this material as well as to optimize the design of these types of smart materials.

Keywords: Shape memory allows; thermomechanics; strain energy; phase transformation; bending and internal forces.

1. Introduction

The Shape Memory Alloys (SMA) [1] metallic materials are relatively new [2] and have remarkable properties for applications of micro-actuators [3] or structures active [5]. They can be used to design mechanical devices "intelligent" [8]. These remarkable functional properties, super-elasticity and shape memory are due to a transformation phase called martensitic transformation between austenite and martensite. This transformation has occurred without volume change is reversible and can be activated either by stress or by temperature [8]. The characteristics of this transformation dramatically depend on the composition of the alloy, its microstructure and hence, the conditions of development and any history of Thermo material [10]. Two principal behaviors have kept out our attention:

*** Correspondingauthor:**NecibBrahim
E-mail: necib15brahim@gmail.com

- The pseudo elastic behaviour is observed when the material is in its phase high temperature (austenite). At constant temperature, the distortions induced under constraints are totally reversible: the charge, austenite is gradually turning into martensite, the landfill is the opposite transformation takes place.
- The one-way shape memory effect is the phenomenon that occurs when SMA regain its original form simply by heating after a deflection at low temperatures. Under this constraint, the material remains in the form martensitic but with a reorientation of platelets martensite.

This work consists on a presentation of an analytical model to conduct load-deformation law characterized analytically then evaluated experimentally. Based on the collected data using numerical model, the strain energy absorbed by these actuators is estimated in the state where the shape memory alloy is present.

2. Materials and methods

2.1 Materials

The material used in this study is an polycrystalline shape memory alloy of TiNi type (50.51 wt% Ti, Ni 49.49 wt%). The tensile testes have been thermally treated. A homogenizing is applied for 2 hours at 870 ° C. An income has been is imposed at 520°C for 30 min and plunged into the water. The transition temperatures determined by differential calorific measure (DSC) are 52°C, 61°C, 48°C, 33°C, 64°C and 78°C for m_f, m_s, r_s, r_f, a_s and a_f, respectively during a cooling and heating.

2.1 Materials

The model reflecting the mechanical behaviour of the SMA is shown in Fig.1 where σ_0 and ε_0 are the stress and the elastic deformation, σ_{max} is the maximum stress which corresponds to a strain ε_{max} recoverable and E_1 and E_2 are the modules of elasticity (Figure 1).

- *Case1:* at $T<m_f$, the alloy is martensitic. A mechanical loading reorients gradually the auto accommodated martensitic up to a noted deformation ε_{max}.
- *Case2:* at $T>a_f$, the SMA is austenite: the deformation does not exceed the value ε_0 beyond which the transformation occurs under stress from austenite to martensitic.

The stress strain relationships for the shape memory alloys are presented as:

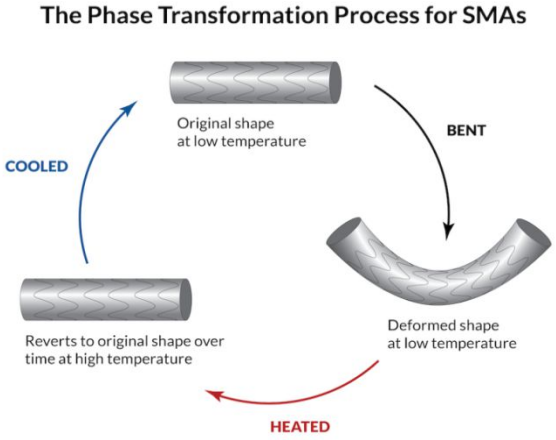

Fig.1 Phase transformation processfor SMAs

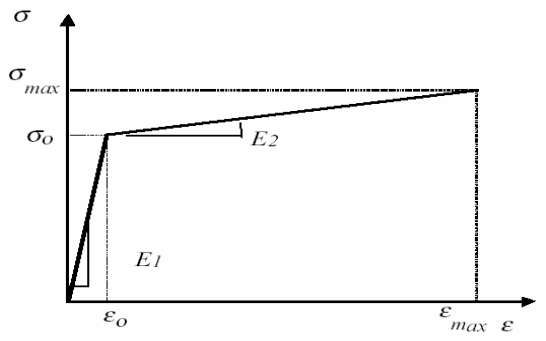

Fig.2 Stress strain relationships for a SMA

On Figure 2, the uni-dimensional stress-strain relationships are theoretically given by the following

equations: $\sigma_A = E_1\varepsilon$ when : $0 < \varepsilon < \varepsilon_0$ (1)

$\sigma_M = \sigma_0 + E_2(\varepsilon - \varepsilon_0)$ when : $\varepsilon_0 < \varepsilon < \varepsilon_{\max}$ (2)

This modelling requires a characterization of these SMA by tests in traction. These tests were carried out using a machine of traction Instron 6025 equipped with a sensor force and an extensometer in order to measure the applied tension and deformation respectively.

3. Mathematical Model

3.1 Shape memory allow response beam in bending

In the case of the bending, the stress distribution is schematised in figure 3.a. This distribution remains linear in the thickness of the sample to the austenitic state ($\sigma \leq \sigma_0$). At ($\sigma > \sigma_0$), a load causes a change of phase in the beam which gives birth of the first appearance of martensitic platelets causing a change in the distribution of stress in thickness (cf.fig.3b). The martensite progresses gradually from the outside to the neutral fibber. This second stage ends at the deformation and stress ε_{max} and σ_{max} respectively, (cf.fig.3c). Beyond this value, a plastic deformation will be present in the sample, which defines other behaviour of the material. In our study, we set our study at the limit of the elastic response of the SMA.

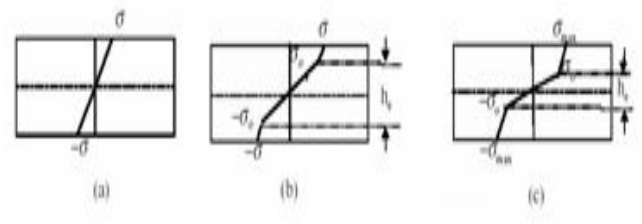

Fig.3 Stress distribution at various stages of loading:

(a) stage1: 100% austenitic

(b) stage2: austenite and martensite

(c) End of stage2 and the beginning of stage 3.

- *Step of loading 1 ($\sigma \leq \sigma_0$) :*

The expression of the bending moment necessary to release the martensitic transformation and the strain energy are given respectively by:

$$M_i = \frac{bh^2}{6}\sigma_0 \quad (3)$$

$$U = 2\int_0^{l/2} \frac{M^2}{2E_1 I} dx \quad (4)$$

The maximum strain energy will be written as:

$$U_i = \frac{6l}{E_1 bh^3} M_i^2 \quad (5)$$

- *Step of loading 2 ($\sigma > \sigma_0$) :*

In this case, M ($M_i < M < M_f$) is the sum of the moments, M_A defines the moment at the heart of the sample (austenitic), and M_M the moment carried out by the skin (martensitic):

$$M = M_A + M_M \quad (6)$$

$$M_A = 2\int_0^{h_e/2} y\sigma_A b dy \quad (7)$$

$$M_M = 2\int_{h_e/2}^{h/2} y\sigma_M b dy \quad (8)$$

Where M_i is the necessary moment for the appearance of the first martensitic plate, M_f is the necessary moment so that the martensitic transformation would be complete, and h_e is the thickness which separates the two areas (austenite and martensite).

The linear distributions of the located stresses in these two regions were obtained respectively as:

$$\sigma_A = \frac{2y}{h_e}\sigma_0 \quad 0 \leq y \leq \frac{h_e}{2} \quad (9)$$

$$\sigma_M = \left[1 + \frac{E_2}{E_1}\left(\frac{2y}{h_e} - 1\right)\right]\sigma_0 \quad \frac{h_e}{2} \leq y \leq \frac{h}{2} \quad (10)$$

These expressions of stresses were obtained by inserting the linear expression of the strain of the sample which is:

$$\varepsilon = 2\frac{\varepsilon_0}{h_e} y \tag{11}$$

From equation 6 and, by combining the equations 7, 8, 9 and 10, the expression of bending moment in the sample (SMA) is obtained in function of the thickness h_e as:

$$M = \left[\frac{h_e^2}{6} + \frac{E_2}{E_1}\frac{h^3 - h_e^3}{6h_e} + \left(1 - \frac{E_2}{E_1}\right)\frac{h^2 - h_e^2}{4}\right] b\sigma_0 \tag{12}$$

The absorbed energy by the beam is obtained by incorporating the energy stored in the nucleus of the beam (austenitic state) and the skin (martensitic state):

$$U = \int_v u dv = 4b\int_0^{l/2} dx\left[\frac{1}{2}\int_0^{h_e/2}\sigma_A \varepsilon dy + \int_{h_e/2}^{h/2}\left(\int_{\varepsilon_0}^{\varepsilon}\sigma_M d\varepsilon\right)dy\right] \tag{13}$$

Substituting the equations 9, 10 and 11 in the equation 12, the expression of energy deformation depending on the thickness h_e is obtained as:

$$U = bl\sigma_0\varepsilon_0\left[\frac{h_e}{6} + (h - h_e)\left(\frac{E_2}{2E_1} - 1\right) + \left(1 - \frac{E_2}{E_1}\right)\frac{h^2 - h_e^2}{2h_e} + \frac{E_2}{E_1}\frac{h^3 - h_e^3}{6h_e^2}\right]$$

Or :

$$U = bl\sigma_0\varepsilon_0\left[\frac{h_e}{6} + (h - h_e)\left(\frac{E_2}{2E_1} - 1\right) + \left(1 - \frac{E_2}{E_1}\right)\frac{h^2 - h_e^2}{2h_e} + \frac{(h^3 - h_e^3)}{6E_1 h_e^2}E_2\right] \tag{14}$$

3.2Shape memory allow response in traction

The model of the absorbed energy by a beam (SMA) exerted under a simple traction has been considered here. We proceed in the similar case cited above. The maximum strain energy which can be absorbed before the outbreak of martensitic transformation caused by the loading (step 1) is:

$$U_i = blh\frac{\sigma_0^2}{2E_1} \tag{15}$$

The strain energy in this second case of loading is:

$$U_i = blh\left[\frac{\sigma^2}{2E_1} + \frac{(\sigma - \sigma_0)^2}{2E_2} + \frac{\sigma_0(\sigma - \sigma_0)}{E_2}\right] \tag{16}$$

Where:б is the applied stress on the SMA beam.

4. Mathematical Model

4.1 Shape memory allow response beam in bending

A series of tests under traction solicitations have been carried out in order to determine the threshold form of the beginning of alloy transformation. We defer here only the necessary results for the continuation of this publication. Figure 4 allows us to compare the experimental stress/strain results and those obtained by modelling. And it appears that a good correlation between the two results and for the two cases was obtained. It is clear to see that at $T<m_f$, the deformation occurred essentially by reorientation of the martensite alternatives characterized change of slope due to the completion of the reorientation process.

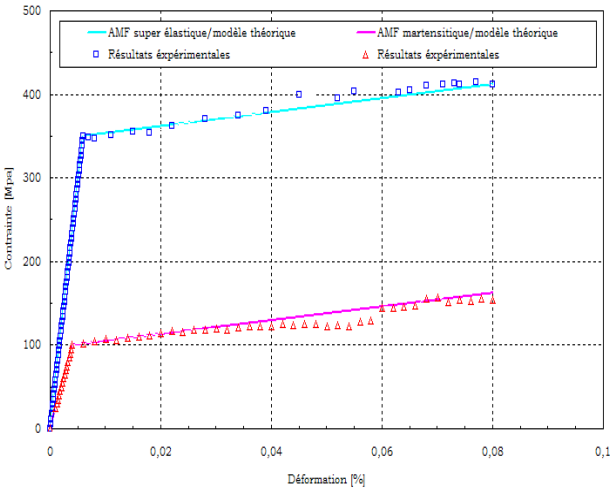

Fig.4 Stress strain curve of SMA after heat treatment

It appears that when $T>a_f$, we observe a limit elastic tree times higher than that measured at $T<a_f$. But, once the loading exceeds that limit, a change of slope is observed which means the beginning of the austeniticmartensitic transformation, and the whole results are presented in Table 1[13].

Table 1: Mechanical properties of the TiNi alloy

Material properties	SMA (super elastic)	SMA (Martensitic)
Young modulus E_1 [MPa]	58334	25000
Young modulus E_2 [MPa]	839	814
Deformation of the beginning transformation ε_0 [%]	0,627	0,385
Stress of the beginning transformation σ_0 [MPa]	354,8	102,8
Deformation of the end of the transformation ε_{max} [%]	8,12	8
Stress of the end of the transformation σ_{max} [MPa]	409	152

4.2 Numerical modelisation results

To modelise the SMA ability of the strain energy absorption, an analytical model has been proposed in order to understand fully their reactions to external applied forces. For this, the simple geometrical parameters and dimensions of the SMA beam at super elastic and a martansitic state are: l = 100mm (length), b = 2mm (width) and h = 2mm (thickness). Also the mechanical properties of this beam are given earlier in Table 1[13].

4.2.1 Case of the SMA in bending

The obtained numerical results are shown in figure 5 which shows that the obtained strain energy is sensibly uncrossing. It appears also that the state of phase of the sample influences on the behaviour of the beam, which is in our knowledge a very interesting result. We observe also that more than the transformation in the beam is important more than the energy is lower. In order to predict in a better way this behaviour, we propose to see in the fallowing the evolution of the bending moment in both cases (fig6).

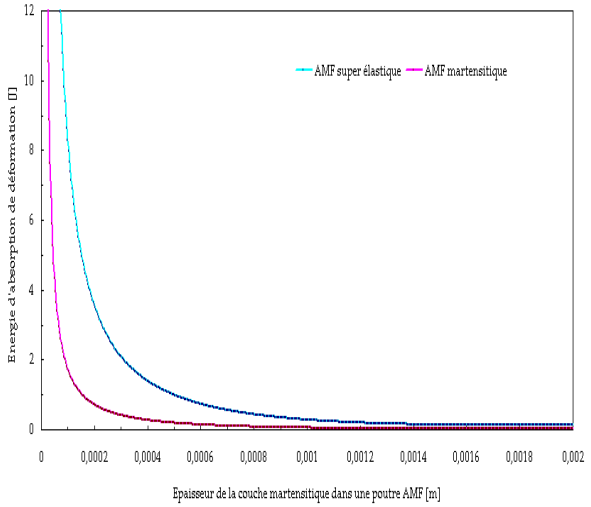

Fig. 5 Energy deformation in terms of martensitic thickness

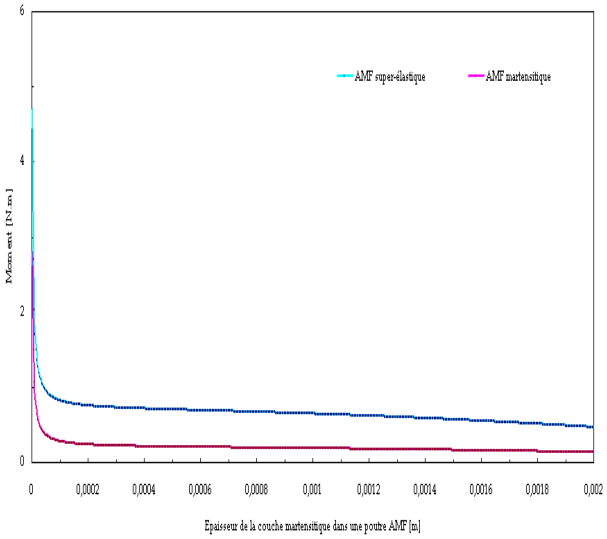

Fig.6 Bending moment in terms of martensite thickness

During loading moment, it appears enough clear similar evolutions in the two phases. Indeed, this moment progresses gradually from outside towards the neutral fibre (Figure 7). The necessary moment to cause the transformation phase in the beam is much

more significant in case 1 than in case 2 (0,58N.m against 0,17N.m). The relation between the deformation energy and the bending moment is represented on Figure 7, where we notice that a faster beginning of deformation energy is noted in a martensitic beam than this of austenitic.

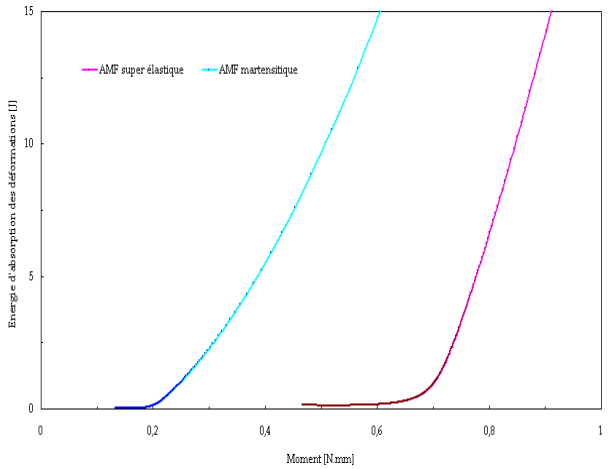

Fig.7 Energy deformation in terms of the bending moment

4.2.2 Case of SMA beam under a traction

The strain energy deformation in terms of the applied axial stress (traction) is represented on Figure 8. It is clear to see that thisstrain energy increases slightly until the applied stress reaches the value of σ_0. Beyond this value, a change of slope is observed. However, the energy deformation is much higher in the case of austenitic that in the case of martensitic beam.

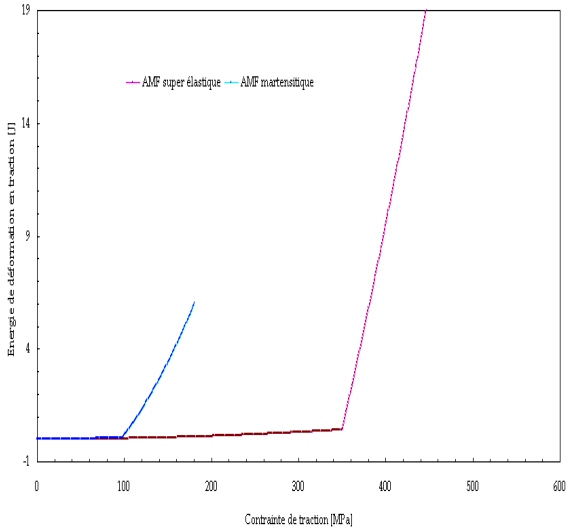

Fig.8 Strain energy deformation in terms of axial stress

6. Conclusions

This work has presented a modelling under external solicitations developed and validated experimentally in the aim of estimating the capacity of a SMA beam to observe the strain energy under the effect of these loadings. The obtained results show that this capacity of absorption energy seems to depend on the phase where the beam is and whatever its type of loading. In order to analyzing these results, characterization tests rather by traction or by DSC have been realized. This enabled us to determine, on one hand, the temperatures of the transformation, the Young modulus and, on the other hand, to validate the model of stress strain behaviour law. It has been noted that the first obtained results are very promising.

The quantification to evaluate the capacity of the SMA to absorb an energy deformation is essential in order to improve the performances of these types of materials known as « smart intelligent ». It allows us also to optimize the concept, the design and the mechanical characteristics of these new materials. This multiplicity of configurations is then necessary to analyse the behaviour of these materials and let foresee a widened field of application for the hybrid composite materials.

References

[1] Patoor E. et M. Berveiller M. Les alliages à mémoire de forme, Hermes, 1990

[2] Ball, P. Made to Measure, New materials for the 21st Century. Princeton, NJ: Princeton University Press, 1997

[3] M. Kohl et al. Development of Microactuators based on the Shape Memory Effect,Proc. Int. Conf. on Martensitic Transformations, Lausanne, 1995, in press.

[4] Spillman W.B. Sirkis J.S and Gardiner P.T. Smart materials and structures: whatare they, Smart Mater.Struct. 1996, (2): 247-254

[5] Foo T.H.E. Active suspensions for flexible-bodied rail vehicles, PhD Thesis, Loughborough, June 2000

[6] Hodgson, Darel E. Et al. Using Nitinol Alloys. San Jose, CA: Shape Memory Applications, Inc., 2000

[7] Sahli M.L. and Necib B. Experimental characterisation and numerical modelling of a pseudo elastic behaviour of Ti-Ni shape memory alloys, International Review of Mechanical Engineering (IREME), ISSN 1970-8734, Vol. 2N.5, September 2008.

[8] Tiberkak R., Bchene M., Rechak S. and NecibB..Damage prediction in composite plates subjected to low velocity impact, Journal of Composite Structures, Marsh 2007.

[9] Mohsin IU, et al. (2012) Finite element sintering analysis of metal injection molded copper brown body using thermo-physical data and kinetics. Comput Mater Sci 53:6–11, (2012)

[10] Sahli M, Gelin J-C, Barriere T. Characterisation and replication of metallic micro-fluidic devices using three different powders processed by hot embossing. Powder Technol 246:284–302, (2013).

[11] A.Lebied, B.Necib, M.Sahli and J-C. Gelin, T. Barrière, Numerical simulations and experimental results of tensile behaviour of hybrid composite shape-memory alloy wires embedded structures, The International Journal of Advanced Manufacturing Technology Int J AdvManufTechnol, Vol. 77, Issue 1-4 December 2015, Springer, London.

[12] A.Lebied, B.Necib, M.Sahli, Analytical Modeling of a Piezoelectric Bimorph Beam, American Journal of Mechanical Engineering, 2016, Vol. 4, No. 1, 7-10, EducationPublishingDOI:10.12691/ajme-4-1-2

[13] S. Yang, C. Wang, Z. Shi, J. Wang, J. Zhang, Y. Huang, X. Liu, Microstructure, martensitic transformation, mechanical and shape memory properties of Ni-Co-Mn In high-temperature shape memory alloys under different heat treatments, Materials Science and Engineering: A, 655 (2016) 204-211.